



A Numerical Investigation on Behavior of Column Base Plates with Different Configurations

Mohamadreza Shafieifar ^{a*}, Vahid Khonsari ^b

^a Florida International University, Department of Civil and Environmental Engineering, Miami, 33174, USA.

^b Sharif University of technology, Department of Civil Engineering, Tehran, Iran.

Received 06 March 2018; Accepted 11 June 2018

Abstract

Base plates are one of the most important types of connections in structures. Due to complicated steel-concrete interaction, simple assumptions of the stress distributions are usually employed for designing the connection. Simple assumptions of compressive stress distribution in concrete may accelerate the design procedure, but they may lead to overdesign results. In this study, six different types of base plates with different configuration were studied numerically using a commercial Finite Element (FE) software and the numerical model was calibrated with an experimental test. The models were subjected to a constant axial load and then a monotonic moment loading was applied. To investigate the effects of the axial load, several axial load level were considered for each configuration. As a result, moment-rotation curves of these base plates, including their rotational stiffness, in the absence and presence of the axial loads, were compared. Moreover, the stress distribution in the concrete was studied in the FE models. For all cases, the stress distribution in the concrete was semi-triangular with the maximum stress between the column flange and the edge of the plate. Based on numerical results, some concepts of simplified assumptions were proposed to find the stress distribution of the base plates. These assumptions are more realistic than current assumptions in structural specifications.

Keywords: Base Plate; Column Base; Concrete Damage Plasticity; CDP; Stress Distribution; Finite Element Modeling.

1. Introduction

Base plates, as particular types of connection, is used to connect the columns to the foundations and distribution of loads. When the column is subjected to a moment, the base plates resists the applied moment by the development of tensile and compressive forces. The compressive force is transferred to the foundation by concrete and the tensile load is carried by the anchor bolts. To distribute the loads of column to the concrete of the foundation on a larger area, a steel plate named base plate can be used.

It is necessary to point that analyzing and determining loads in the structures are related to its boundary conditions, and base plates as the support of the structures, may affect the calculated forces. On the other hand, to design a base plate, applied loads should be known. This means primary design and analysis of the structures are related and an iterative procedure must be employed to achieve an economical and safe design. Therefore, determination of the resistance and the behavior of the base plates are important based on the following reasons: 1) Determination of the base plate rotational stiffness represents the support conditions that have a significant effect on the load distribution. 2) The rigidity of the base plate influences the total displacement and drift of the structure and wrong estimations may cause exaggerated deformations. 3) Effective length and consequently the critical load of the columns in the first floor is a

* Corresponding author: mshaf017@fiu.edu

 <http://dx.doi.org/10.28991/cej-0309169>

➤ This is an open access article under the CC-BY license (<https://creativecommons.org/licenses/by/4.0/>).

© Authors retain all copyrights.

function of the support conditions.

In many circumstances, the traditional assumption of considering base plates as either 'Rigid' or 'Hinged,' is not realistic. If a non-rigid connection is assumed rigid in the design process, it may cause more drift in practice. On the other hand, when the base plate is rigid but assumed hinged, it may transfer the indeterminate loads to the foundation which it is not designed for.

The simplest base plate includes a plate welded directly to the end of the column and the plate connected to the foundation by anchor bolts. In the absence of the moment in a base plate, the compressive stress is assumed to be uniform and the designing procedure is simple. When a base plate is subjected to a moment, the rotational rigidity is important. To increase the rigidity of the base plates, some attachments can be added but it complicates its behavior even more. Some of the complexities are the interaction between steel and concrete, load contribution of attachments as well as estimating the stress distribution under the base plate.

Dimensions of bolts, plates, and attachments have a significant effect on the base plate rigidity [1]. In common procedure of designing base plates, if the plate is considered completely rigid and the bolts are strong enough, stress distribution in concrete under the base plate is assumed linear, while most base plates are not completely rigid

Figure 1 shows the relation between the support rotational rigidity and the critical load of the columns for different boundary conditions. In this Figure, E , I and l are the modulus elasticity, moment of inertia and the length of the column and K_r is the rotational stiffness of the connection. Considering these figures, the critical load of the columns increases according to the base plate rotational stiffness. Therefore, calculation of the critical axial load is related to the stiffness of the base plate and as it will be shown in this study, the stiffness of the connection is affected by its axial load. Accordingly, both the critical load and the corresponding rotational stiffness should be controlled and the design procedure will be iterative.

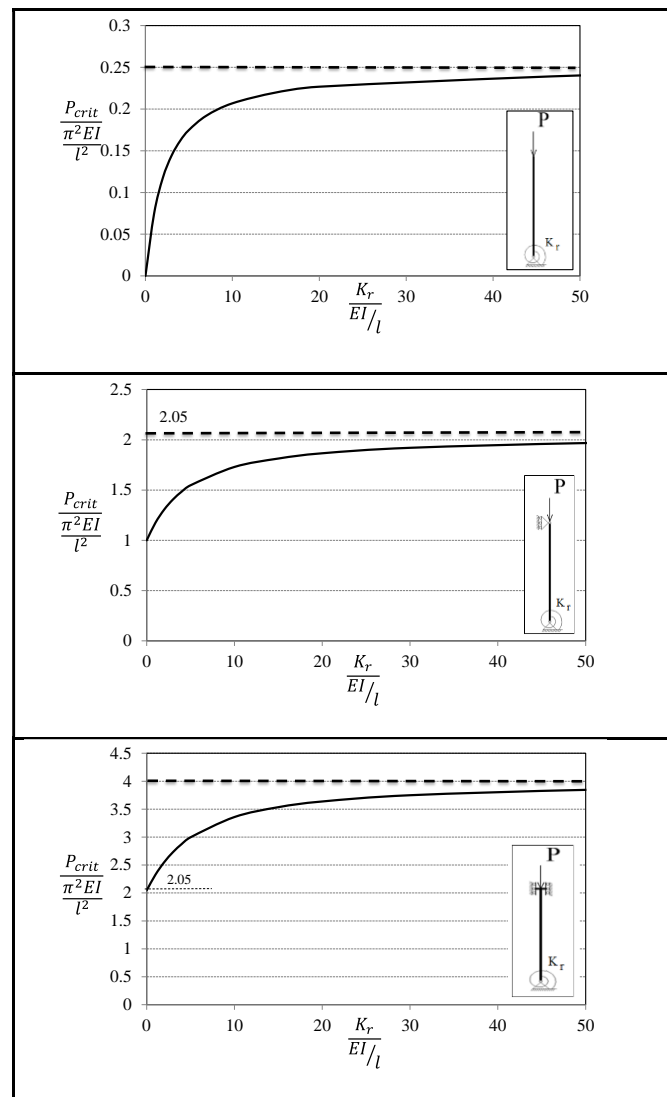


Figure 1. Effect of rotational stiffness on critical load for columns with three different support conditions

Many researchers have investigated base plates both theoretically and experimentally [2-4] but most of them have studied simple cases of base plates including one plate at the end of the column and some of them include stiffeners [5]. Melchers [6] tested several nominally 'pinned' base plate connections. He presented a simple mathematical model for the prediction of elastic stiffness of the connection. Kontoleon et al. [7] have studied on the numerical model of the structural response of a steel column base plate under static loading and two-dimensional Finite Element (FE) model was used to analyze the influence of thickness and the axial load on the base plate performance. Ermopoulos [8] proposed a simple formula between the moment and the rotational stiffness of the base plates. In addition, all necessary coefficients of this formula were given for different cases. Base plate parameters such as stiffness, capacity, and ductility were indicated in moment-rotation ($M-\theta$) characteristics of bolted or bolted/welded connections. In another research, he verified the mathematic formula with experimental results [9]. Dunai et al. tested end-plate-type steel-to-concrete mixed connections under combined compressive normal force and cyclic bending. The main focus of the research was on the rotational stiffness of the mixed connection and its cyclic deterioration [10]. Results of the rotational stiffness and the concepts can be used in base plates designing procedure. In addition to the aforementioned studies, some studies have been conducted on base plates and columns with various shapes such as hollow sections [11-13]. Moreover, several experiments and numerical investigations have been carried out to show the behavior of base plates [14-17]. Beside conventional connections, embedded column base (ECB) [18] and rocking damage-free column base for mid to high rise steel frames [19, 20] has been emerged.

Generally, it can be concluded that if the axial load is large and compressive, then the strength of the concrete in the foundation is the most important factor, but this is not the case for columns with light axial loads compared to applied moment. In this case, the holding-down anchor bolts and the rigidity of the plate are the main factors. The shear force can be transferred by the friction between the plate and the concrete or external shear transmission elements. Some studies over stress distribution on concrete are available in [21, 22].

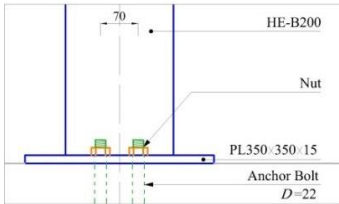
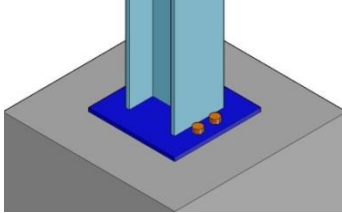
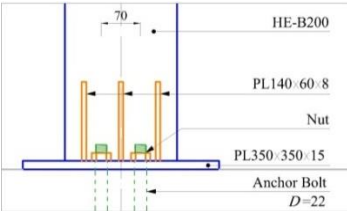
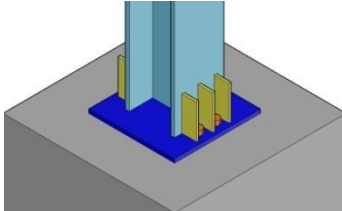
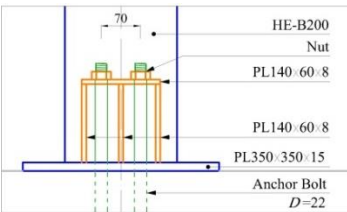
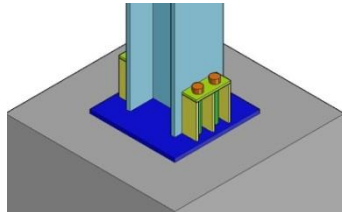
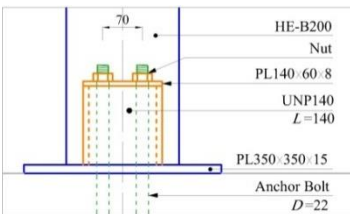
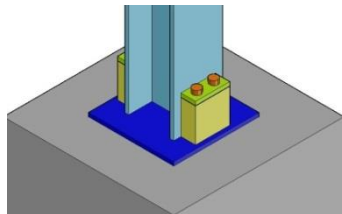
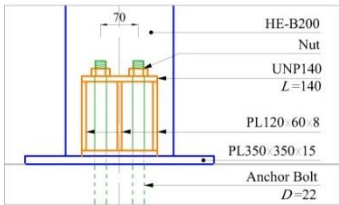
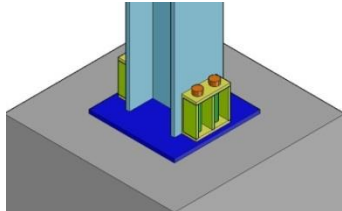
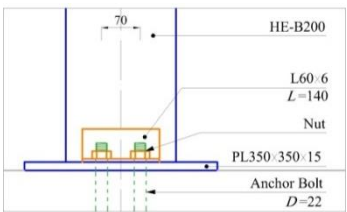
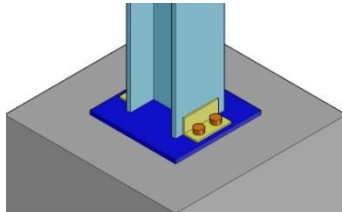
The focus of the current research is to compare different types of the base plate with various attachment. To achieve this goal, six types of base plates with different attachments, which are common in practice, were simulated and compared. The connections, first were subjected to a constant axial load and then a monotonic lateral load was applied. The simulations were performed for different axial load level to investigate the axial load effect on the behavior of the connection. For clarifying the difference between the models, deformation, stress distribution in concrete under the base plate and the moment-rotation curves with different axial loads were investigated.

2. General Configuration and the Geometry of the Studied Base Plates

In this study, six widely-used base plates were considered. These base plates are generally assumed as a rigid or semi-rigid connections. Column, base plate, and the anchor bolts in all models had the same material and geometry and some attachments were added to each type. HE-B 200, based on EuroNorm 53-62 [28] or DIN 1025 [28], a wide flange I section with moderate unit weight was the section of columns. Base plate dimension was $350 \times 350 \times 15 \text{ mm}^3$ and the diameter of anchor bolts was 22 mm. Base plates were connected to a concrete block by four anchor bolts and columns were placed in the center of the base plates. Dimensions of concrete blocks were $700 \times 700 \times 400 \text{ mm}^3$. Bolts spacing along the column flange was 70 mm. Details and schematic drawings of all models are shown in Table 1. The design of the reference connection (model 1) met the minimum requirements of AISC [29].

The first type was the simplest type in which the column was directly connected (welded) to the base plate. In the second model, to increase the rigidity of the connection, three plates were added to the flanges of the column. The dimensions of the plates were $140 \times 60 \times 8 \text{ mm}^3$. The third type was almost the same as the second one but a plate was used on the top of the three stiffening plates and nuts were placed on top of this plate. In the fourth and the fifth models, channel sections, UNP140, based on EN 53-62 [28], were added to increase the rigidity of the connection. These channels were 140 mm long. In the fourth model, a plate was placed on top of each channel and in the fifth, three plates were used as the stiffeners inside the channels. In the fifth model, the two channels with additional stiffeners are welded to the column flanges to transfer the forces to the hold-down bolts [30]. The sixth model includes two angles and usually assumed as a hinged connection in practice. In this model, the column is not connected (welded) to the plate.

Table 1. Details and schematic drawings of the simulated models

Model 1	
	
Model 2	
	
Model 3	
	
Model 4	
	
Model 5	
	
Model 6	
	

3. Numerical Modeling

3.1. Material Properties

The material of the columns, base plates, and attached plates were assumed to be St37 with a yielding stress of $f_y = 240 \text{ N/mm}^2$. The yield stress of the anchor bolts was $f_y = 400 \text{ N/mm}^2$. Concrete Damage Plasticity (CDP) in Abaqus was employed to simulate the concrete material and the nominal compressive strength of the concrete was assumed as

$f'_c = 24 \text{ N/mm}^2$. More details about CDP and nonlinear modeling in Abaqus are available in literatures [32-38]. Elastic and plastic properties of concrete and steel in tension and compression were included in the models. Stress-strain curves of the simulated models are shown in Figures 2-4.

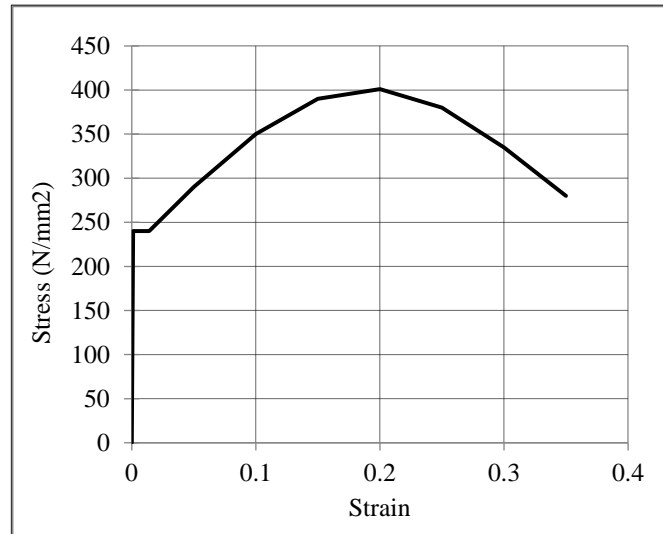


Figure 2. Stress-Strain curve of the material of the columns and plates

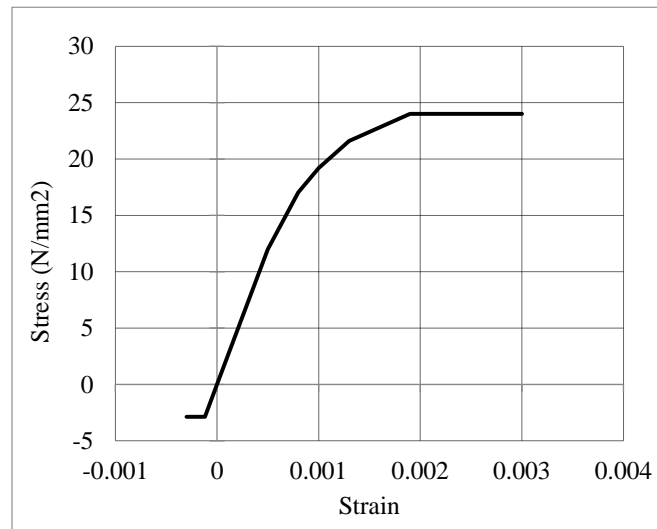


Figure 3. Stress-Strain curve of the concrete material

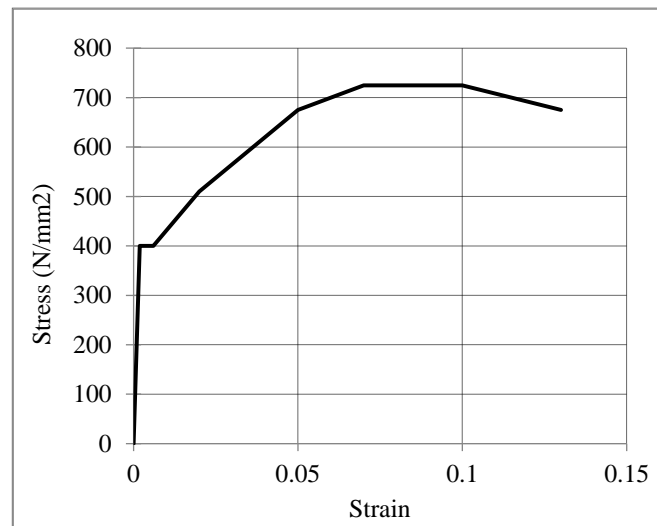


Figure 4. Stress-Strain curve of the material of anchor bolts

3.2. Finite Element Models

Due to the symmetry of the connections, half of them were simulated in the FE model. The bottom of the concrete blocks and the anchor bolts were completely fixed. The interaction between the concrete and anchor bolts was modeled by 'friction' based on studies by others [39]. Eight-node elements (C3D8R) were used to mesh the concrete, anchor bolts, nuts and column section. Mesh arrangement of the model is very important to achieve accurate stress distribution while maintaining reasonable analysis time. The mesh size in crucial regions of the model such as near bolts and column corners was selected small enough, enabling the model to accurately simulate large deflections and stress concentrations. At the same time, to reduce the analysis time, a larger mesh size was used in middle of the base plate and further end of the concrete footing. All models were subjected to a constant axial load and direct moment was applied to the column. To measure the rotations of the connections, the section 200 mm above the concrete block was considered (see Figure 5). In FE models, welds were not simulated and elements of the parts, which are normally welded in practice, were tied together. Some researches modeled welds and investigated the effect of welding on the behavior of the connection [26, 27].

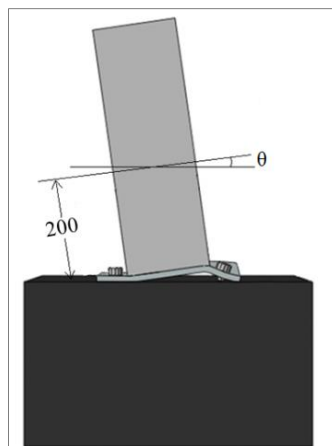


Figure 5. Measurement of rotation (θ) of the connection in the FE models based on the approach adopted by R. Melchers [6]

3.3. Validation of FE Models

To validate the FE modeling details, an experimental test results conducted by Melcher [6] was employed. Specimen (L8) that was tested in 1992 by Melchers was modeled in FE software. He tested 10 specimens without axial force and used 200 UB 25 section as the column. A simple test setup with a reinforced concrete block, representing the foundation, was used for the experiments. The base plates connected to the concrete block with four (or two) anchorage bolts and the concrete blocks clamped to the laboratory strong floor. The base plates were welded to a 100-mm long column with 6-mm fillet welds all around. The lateral load was applied using a hydraulic ram and the applied load was measured using a calibrated load cell. The rotation of the column was measured at 200 mm above the base plate [1, 6]. The simulated specimen (L8) in the current study, was connected to the concrete block by four anchor bolts. The diameter of anchor bolts was 12 mm and dimension of the base plate was $300 \times 200 \times 10 \text{ mm}^3$.

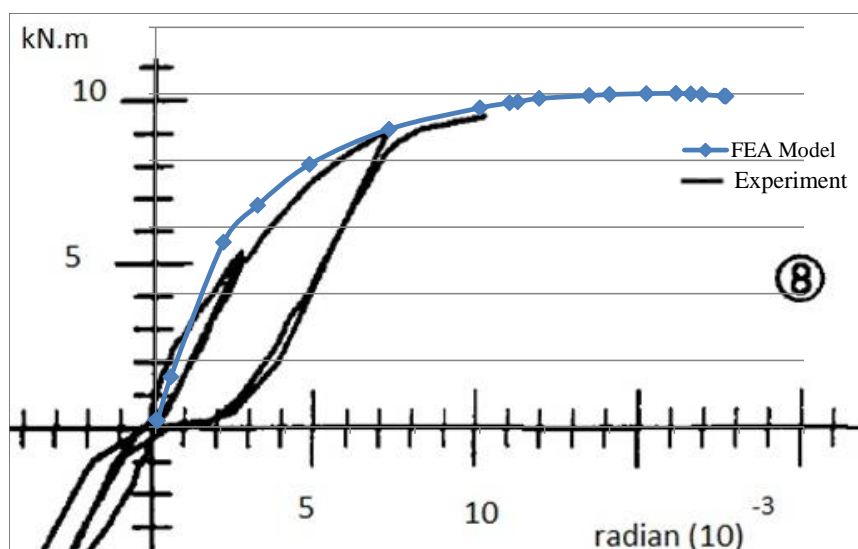


Figure 6. Comparison between the experimental [6] and numerical (FEA) results

This model was simulated according to the existing information of the material properties and loading conditions. To compare the results of the experimental results and the FE model, moment-rotation ($M-\theta$) curves are shown in Figure 6. The FE results indicate that there is a good agreement between experimental and numerical results. The existing correlation between these curves is an indication of the correct modeling of the system, including the material properties and the interactions between materials.

4. Results and Discussion

4.1. Failure Modes of the Studied Models

Exaggerated deformations of the models at their last stages (35×10^{-3} rad. rotation) are shown in Figures 7-12. In the first model, excessive bending of the base plate cause large deformation in the connection. In this model, the critical zone was located just next to the flange of the column. In the second model, the large deformation of the holding-down bolts was the cause of overall failure. In this model which had the most rigidity, the column reached its capacity and had large deformations in the flanges but the angel of the column and base plate remained orthogonal. In the third model, the plate that was placed on top of the stiffeners, deformed in small moments and the connection was unable to transfer larger moments. It seems that this connection, with the current design, cannot be considered as a rigid one. Failure of the fourth model was started with large deformation of the channel web. In the fifth model, the flange of the channel was the most vulnerable element.

Generally, it seems that in the connections with the nuts placed above a plate (Models 3, 4 and 5), the plate that the nuts seat on, had a significant effect on the stiffness and a flexible plate made the anchor bolts useless. The advantage of these connections is related to the designing of the welds. In these cases, welds are either under pressure or sheer. In the sixth model which is assumed as hinge connection in practice, and is one of the most common connections in the structures, angels were the weakest part. In all models, tension part of connections was more vulnerable than the compressive parts.

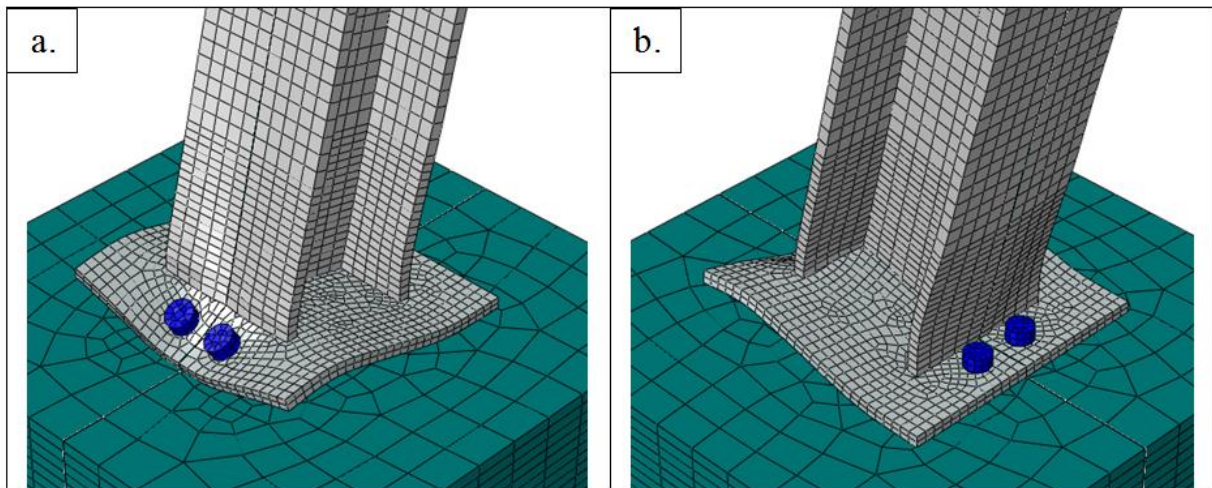


Figure 7. Deformation of model 1. a) Tensile flange, b) Compressive flange

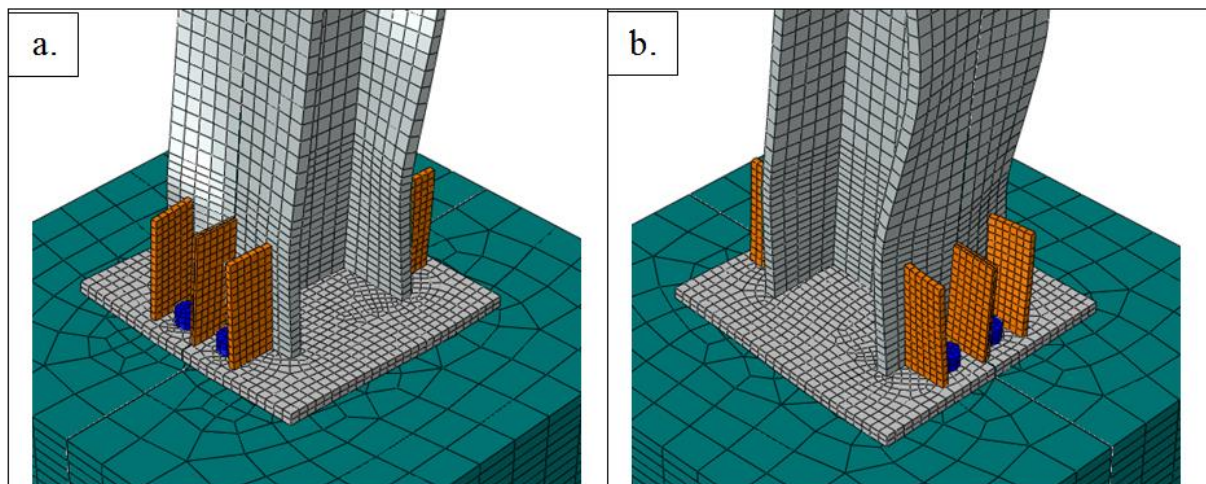


Figure 8. Deformation of model 2. a) Tensile flange, b) Compressive flange

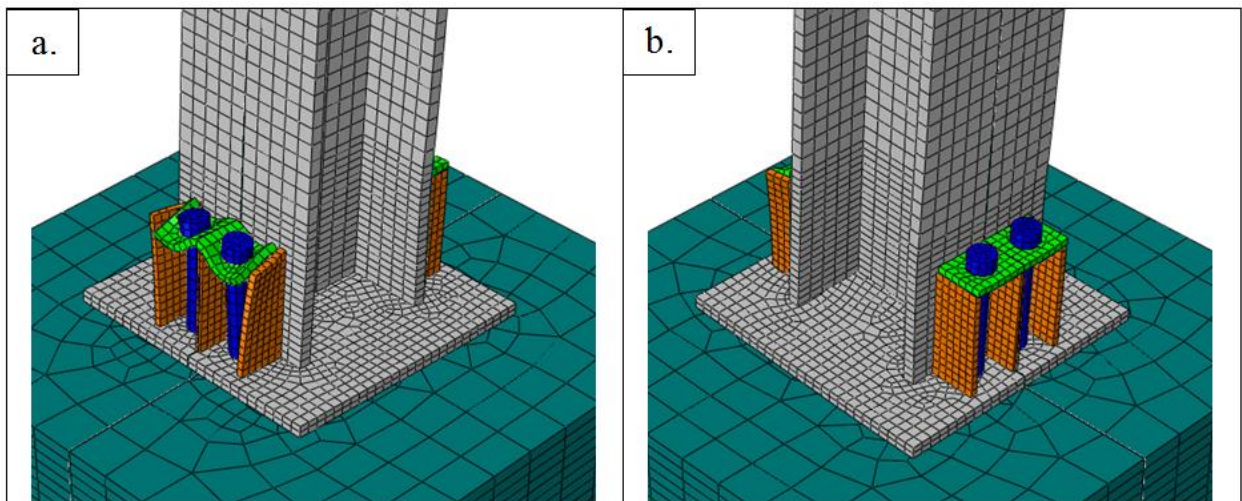


Figure 9. Deformation of model 3. a) Tensile flange, b) Compressive flange

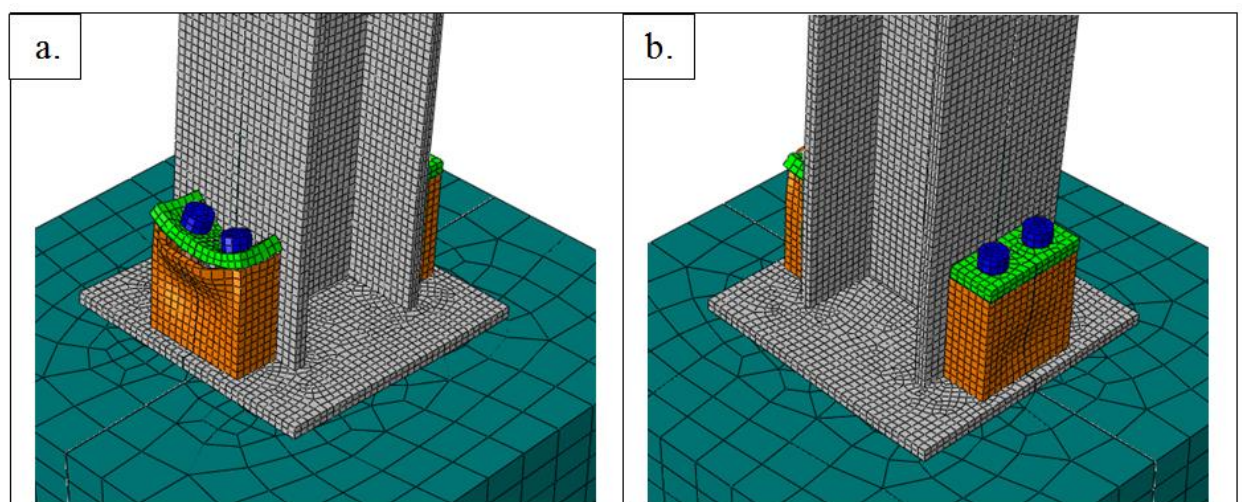


Figure 10. Deformation of model 4. a) Tensile flange, b) Compressive flange

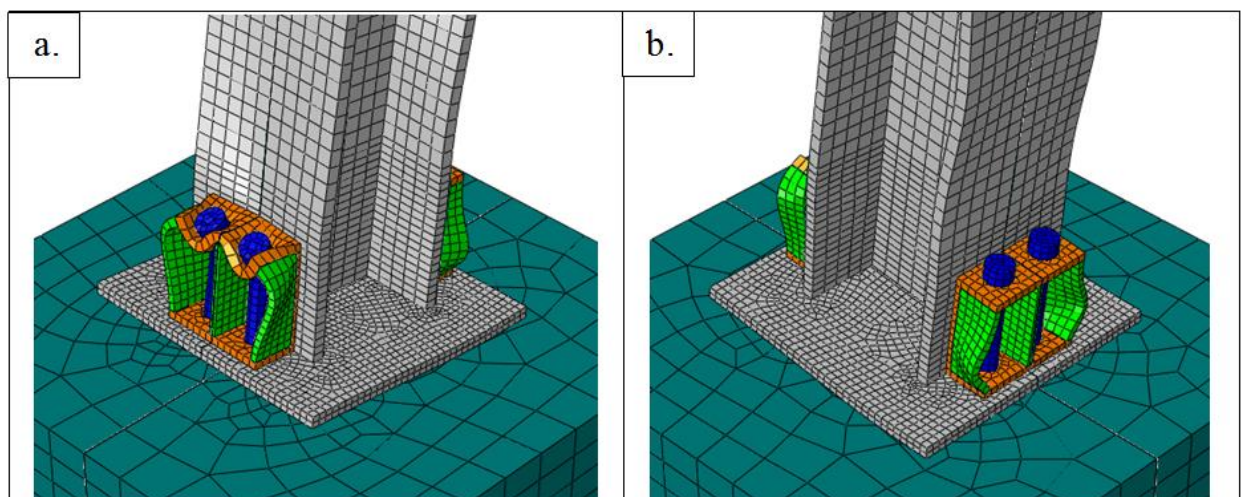


Figure 11. Deformation of model 5. a) Tensile flange, b) Compressive flange

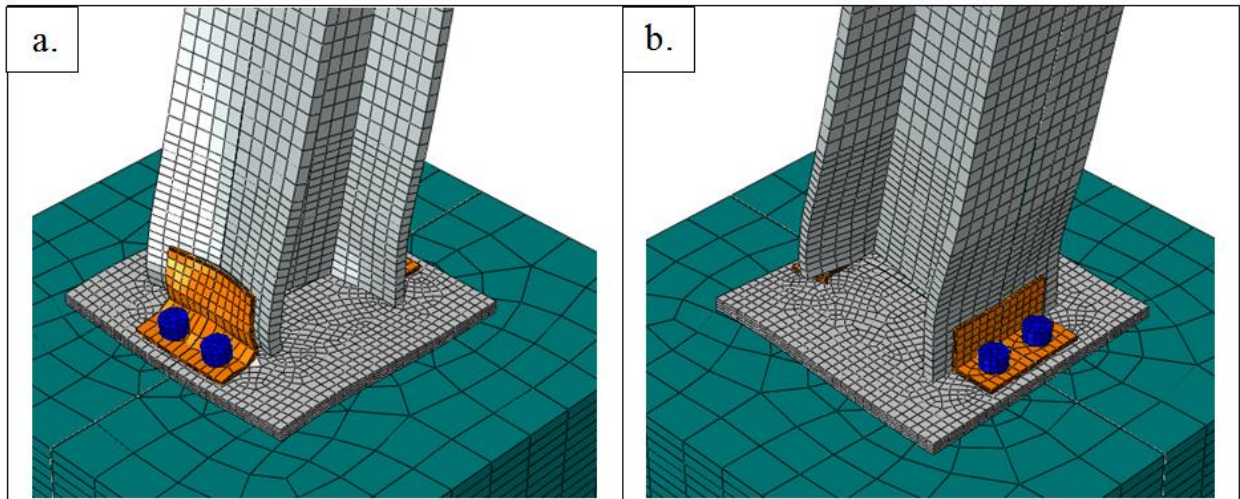


Figure 12. Deformation of model 6. a) Tensile flange, b) Compressive flange

4.2. Stress Distribution inside Concrete Foundation

Stress distributions in the concrete under 50 kN.m moment with different axial loads are shown in Figures 13-18. In these figures, P_y is the pure axial load capacity of the column section ($P_y = A_{\text{column}} \times f_y$) and P represents the axial load. The maximum stress zone was different in the models. In the first model, the maximum stress occurred just below the flange of the column in compression. In the second model, with the largest inelastic stiffness, and in the fifth model, the maximum stress was located between the bottom of the flange of the column in the compression and the end of the base plate. In the third and the fourth models, the maximum stress occurred at the end of the base plate. The stress distribution at the height of the block in models 1 and 2 then 3 and 4 were similar.

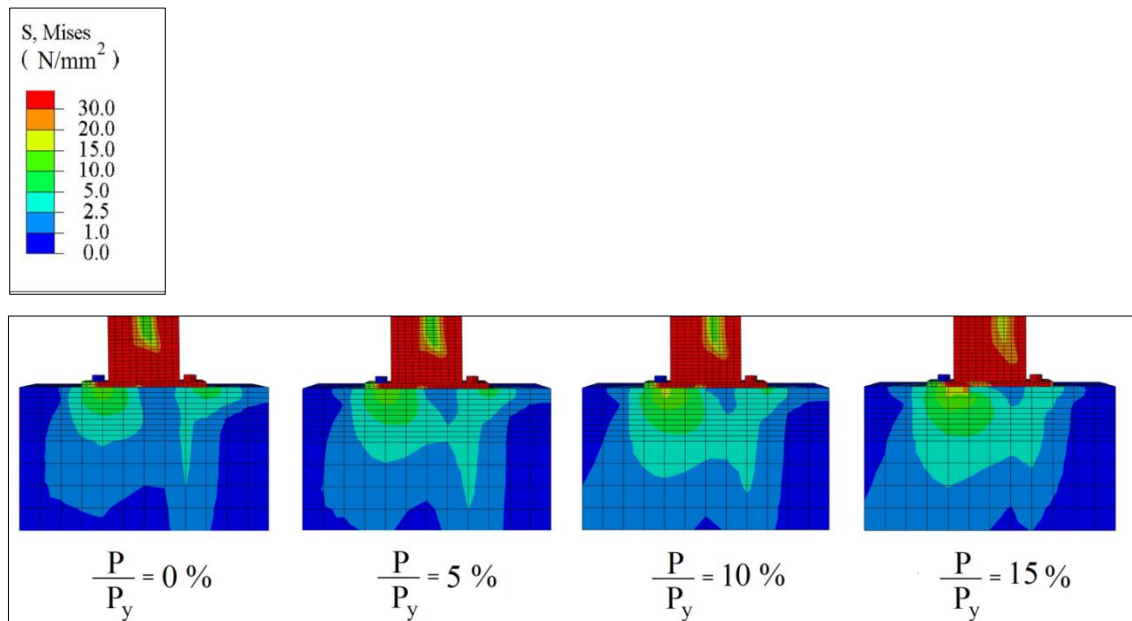


Figure 13. Stress distribution of model 1 inside concrete with different axial loads

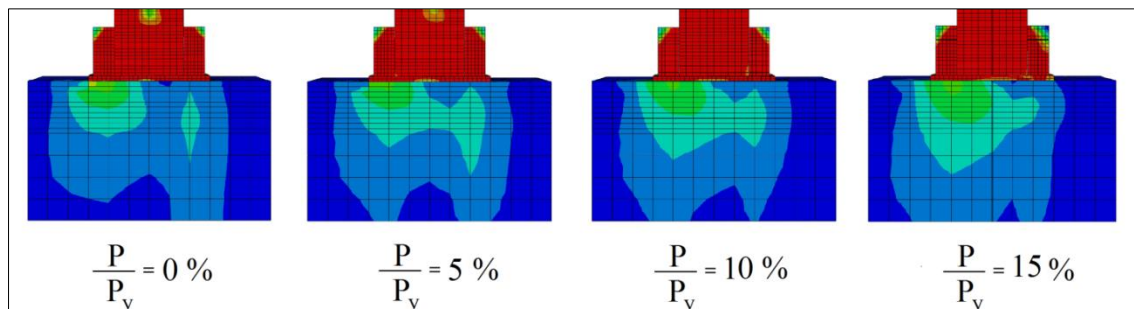


Figure 14. Stress distribution of model 2 inside concrete with different axial loads

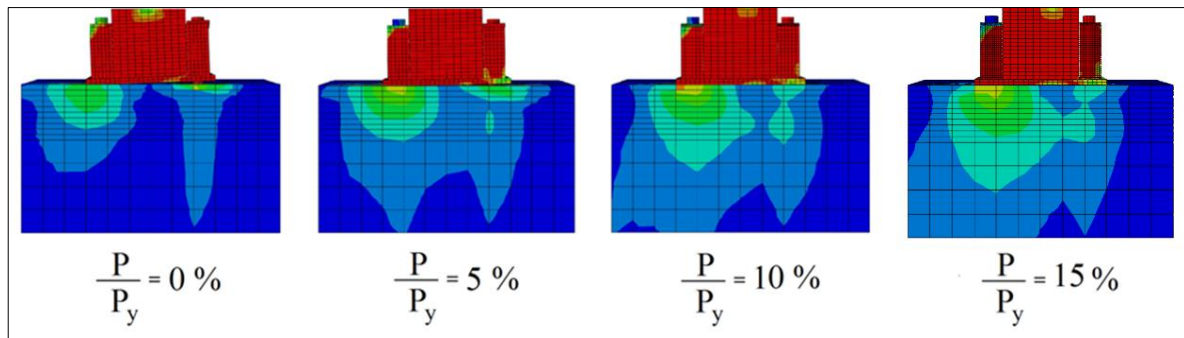


Figure 15. Stress distribution of model 3 inside concrete with different axial loads

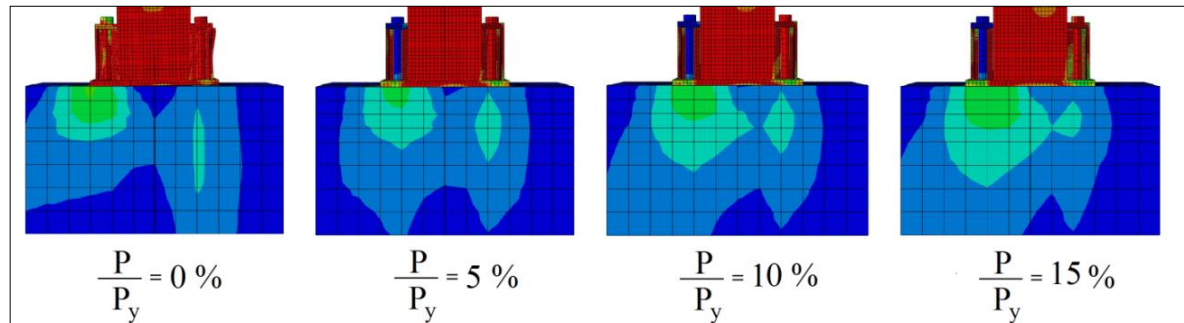


Figure 16. Stress distribution of model 4 inside concrete with different axial loads

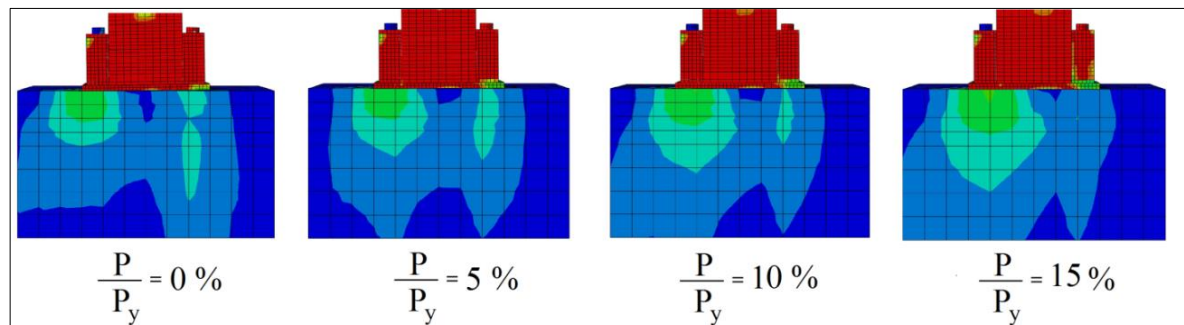


Figure 17. Stress distribution of model 5 inside concrete with different axial loads

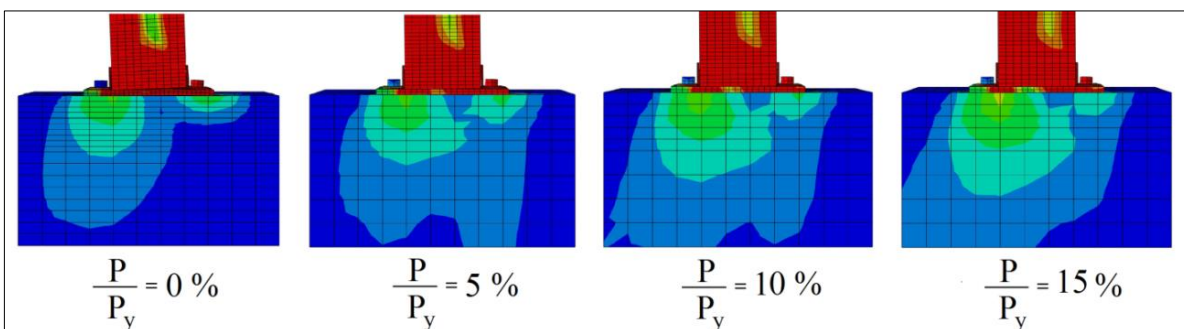


Figure 18. Stress distribution of model 6 inside concrete with different axial loads

4.3. Moment-Rotation ($M - \theta$) Curves

The initial stiffness of the connections is calculated using the slope of their $M - \theta$ curves at $\theta = 0$. In Figure 19, the curves of $M - \theta$ for the simulated models in the absence of axial force are compared. Model 2 had the largest stiffness. In model 3, the large deformation of top plate was the cause of initial stiffness reduction. However, the ultimate capacity of model 5 was greater than those of others except model 2, while its stiffness (K_e) was less than those of models 1 and 4. In Figures 20-25 the curves of $M - \theta$ for all the models with various axial forces have been plotted. Increasing the axial loads reduces the tension in the anchor bolts and this causes the base plate to be pressed against the concrete block and have a lower rotation. In model 2, in the case of the existence of axial force, the capacity of the connection was

equal to the plastic moment of the column section. In models 3 and 4 even with a minor amount of axial force ($P/P_y = 5\%$), rotational stiffness was increased considerably. In models 4 and 5 when ($P/P_y = 10\%$), as the moment was increased, the compressive part was considerably deformed; therefore, their stiffness was less than when ($P/P_y = 5\%$).

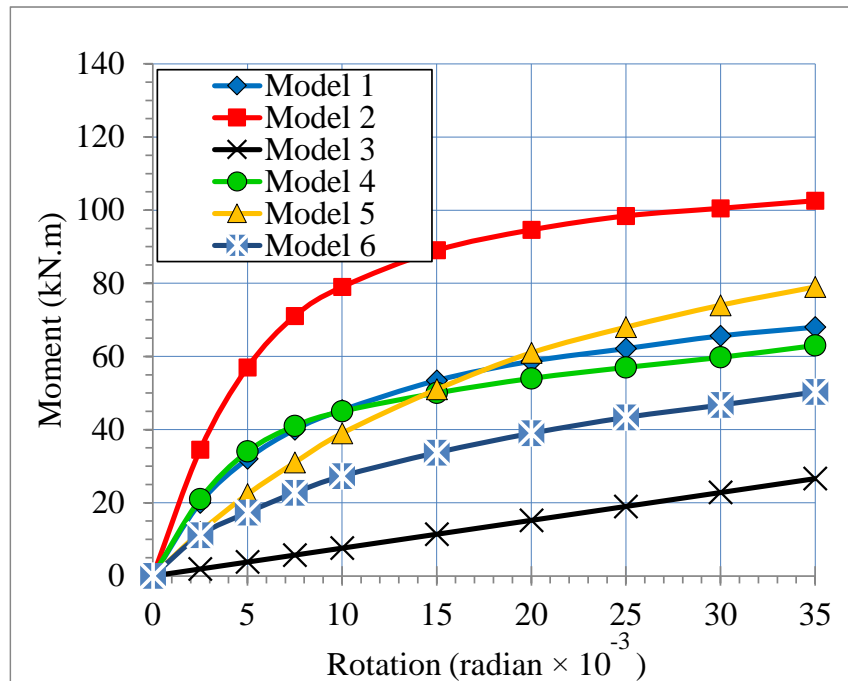


Figure 19. Moment-Rotation curves of the studied models without axial force ($N=0$)

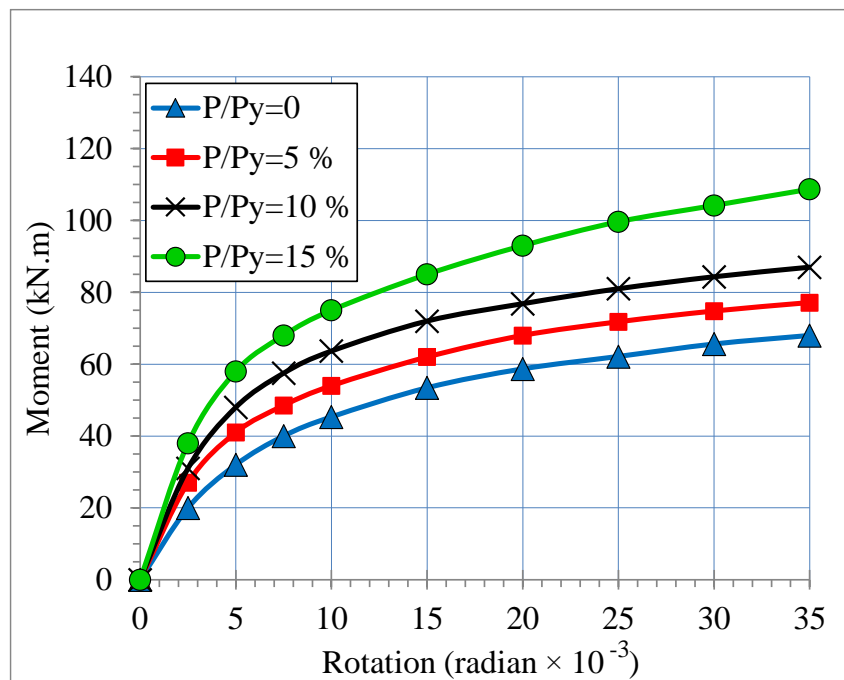


Figure 20. Moment-Rotation curves of model 1 with different axial force

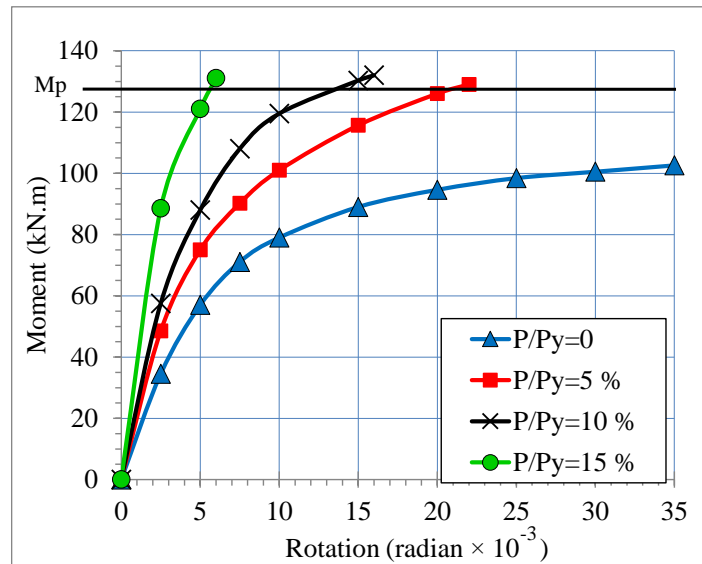


Figure 21. Moment-Rotation curves of model 2 with different axial force

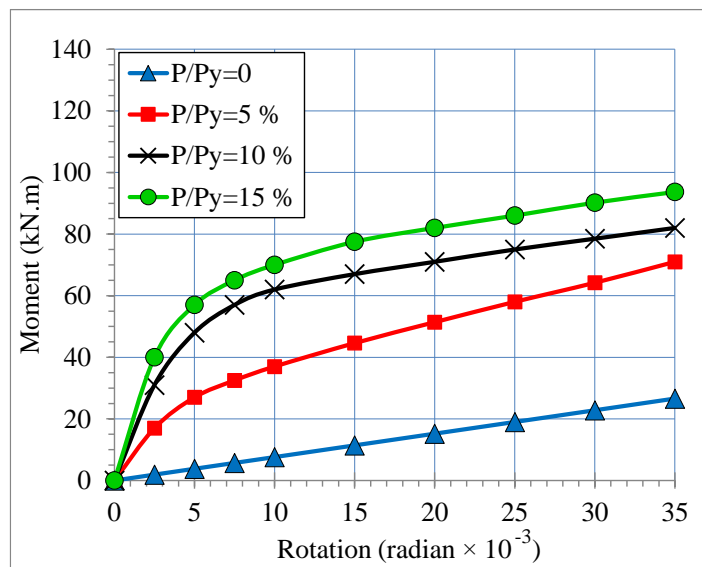


Figure 22. Moment-Rotation curves of model 3 with different axial force

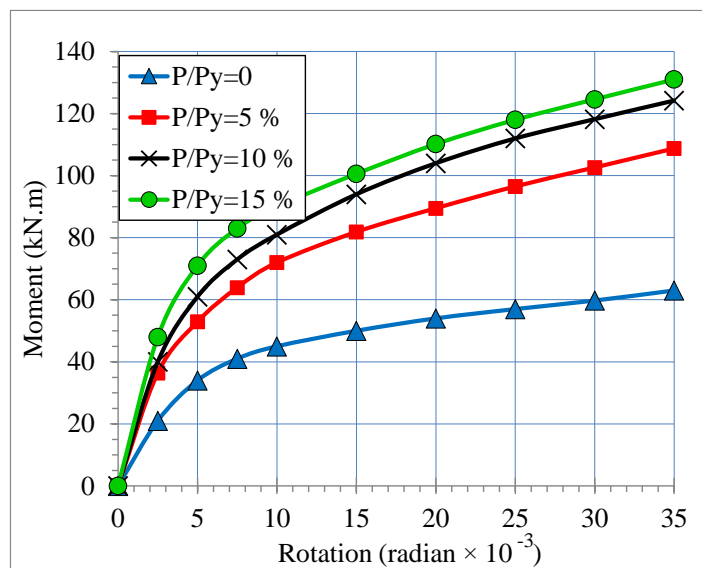


Figure 23. Moment-Rotation curves of model 4 with different axial force

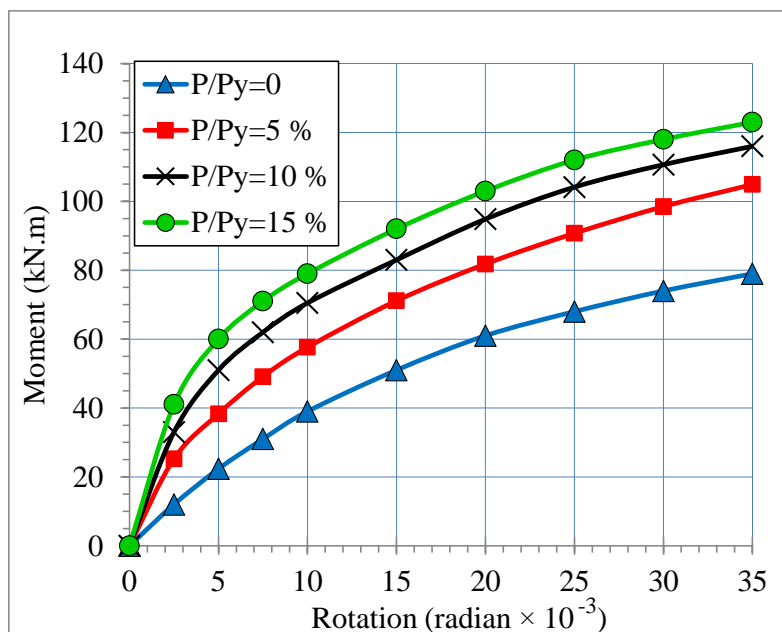


Figure 24. Moment-Rotation curves of model 5 with different axial force

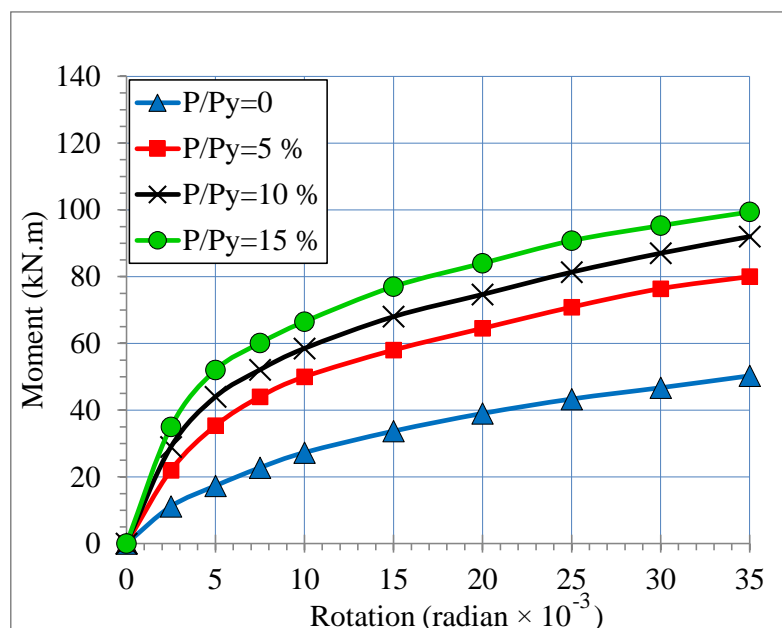


Figure 25. Moment-Rotation curves of model 6 with different axial force

The rotational stiffness of the models presented in Figure 26. The second model while $P/Py = 15\%$ had the largest rotational stiffness with a noticeable difference. Even though model 6 was considered as a hinge connection, its rotational stiffness in $P/Py = 15\%$ was more than the rotational stiffness of the stiffest model (Model 2) in the absence of axial force. Rotational stiffness of models 1, 3, 4 and 5 at $P/Py = 15\%$ are close to each other, however, if the welds were modeled it could possibly change the results.

According to Figure 26, it is possible to figure out that the axial force had a noticeable effect on rotational stiffness. For example, in model 2 rotational stiffness in ($P/Py = 15\%$) in the case of the absence of axial force was almost doubled. As it was mentioned in the introduction, the critical axial load is a function of the rotational stiffness of the supports. According to AISC, when $K_e l/EI$ is less than 2 the connection should be considered as a hinge. To estimate the effect of the axial load on rotational stiffness and its counter effect on the critical axial force, Figure 27 has been illustrated for a column with a normal length. Regarding the Figure 27 and 1, the critical load can be calculated for each case.

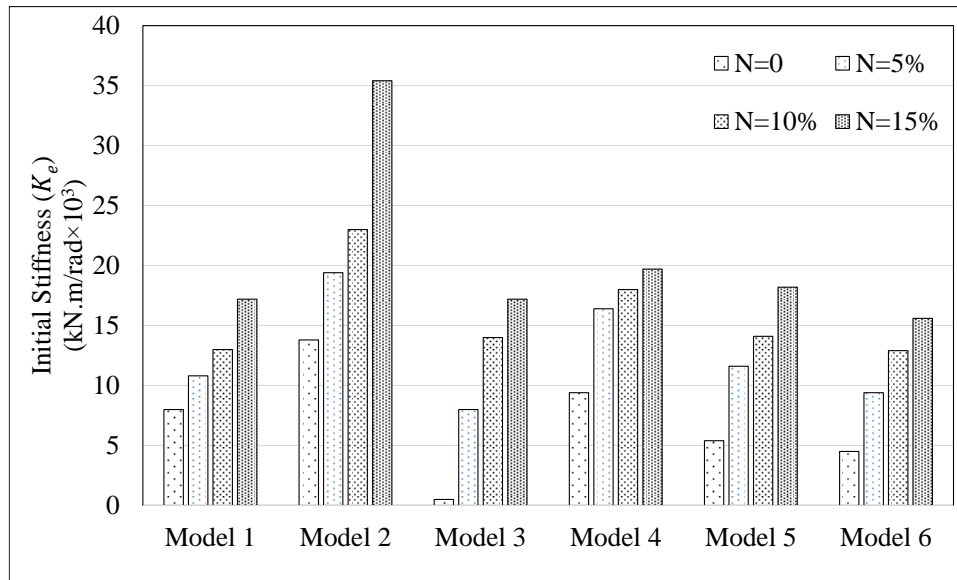


Figure 26. Initial stiffness of various models subjected to different levels of axial load

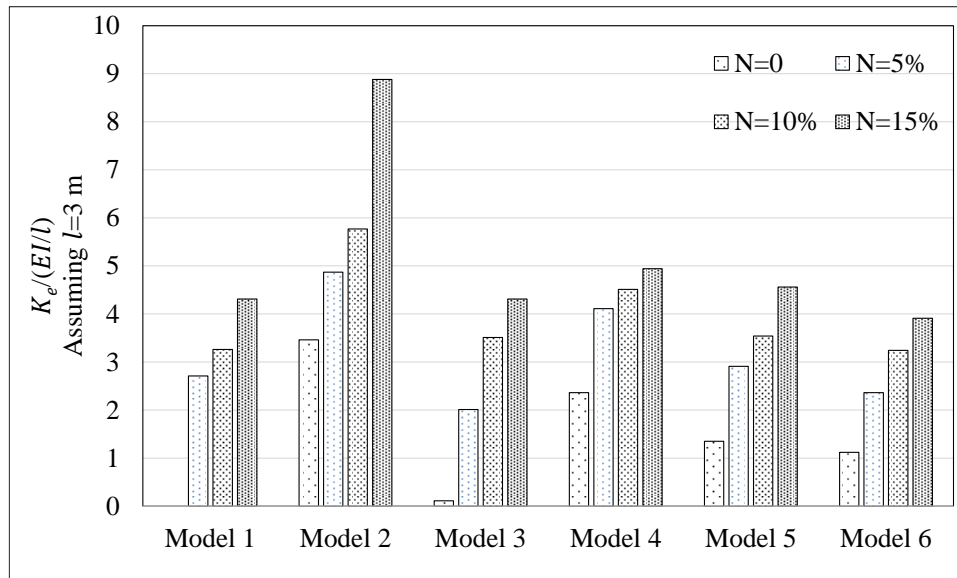


Figure 27. Ratios of initial stiffness of modeled base plates to those of their columns

4.4. Stress Distribution

To achieve the accurate stress distribution under a simple base plate, a base plate was designed for a column with a HE200-B section, axial force of 400 kN and moment of 80 kN.m, based on AISC. The dimension of the plate calculated as $350 \times 350 \times 40$ mm³. Then the column and the base plate were simulated in FE model. The material properties of this model were the same as introduced in numerical section. Figure 28 shows a comparison of stress distribution in the concrete between the FE model and some of the common methods for base plates designing.

As it is obvious, on the contrary to the theory of the proposed methods, the highest stress in this base plate was underneath the compressive flange. Of course, it is clear that one of the major differences among the common methods and FE model is related to the way in which stress is distributed on the width of the base plate. In the mentioned methods, stress distribution on the width of the base plate is considered constant while this does not apply to reality nor FE model.

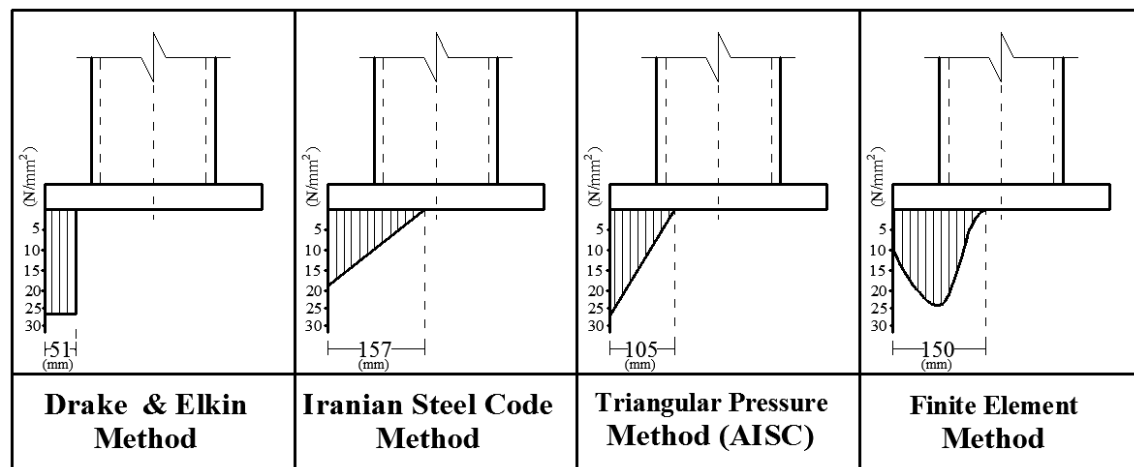


Figure 28. Distribution of contact stresses under base plates obtained based on different methods

5. Conclusion

The study carried out in this research is based on the numerical studies. However, an experimental work is required to complement the results reported here. Within the context of the results obtained in this work, the following conclusions can be drawn.

- The effect of axial force on rotational stiffness in all the models was considerable. For instance, the rotational stiffness of the models with a high level of axial load ($P/P_y=15\%$), was more than twice of those without axial load ($P/P_y=0\%$).
- In circumstances where the anchor bolts were connected to the system through an added top plate (models 3 and 4), such plates were most vulnerable elements in the system. Besides, such configuration had an adverse effect on the rigidity as well as the moment capacity of the connection. Apparently, increasing the thickness of such plates may increase the rigidity and the capacity of the connection.
- With moderate sized added top plates in model 3, the designed connection cannot be considered as rigid one. Amongst all studied base plates, model 2 had the highest, and model 3 had the lowest rigidity.
- Employing models 4 and 5 results in better stress distribution in the concrete.
- For semi-rigid base plate, the highest stress was underneath the compressive flange.

6. References

- [1] Hon, K.K., and R.E. Melchers. "Experimental Behaviour of Steel Column Bases." *Journal of Constructional Steel Research* 9, no. 1 (January 1988): 35–50. doi:10.1016/0143-974x(88)90055-7.
- [2] Lee, Dae-Yong, Subhash C. Goel, and Bozidar Stojadinovic. "Exposed column-base plate connections bending about weak axis: I. Numerical parametric study." *International Journal of Steel Structures* 8, no. 1 (2008): 11-27.
- [3] Turvey, G.J., and C. Cooper. "Semi-Rigid Column-base Connections in Pultruded GRP Frame Structures." *Computers & Structures* 76, no. 1–3 (June 2000): 77–88. doi:10.1016/s0045-7949(99)00143-1.
- [4] Penserini, Paul, and André Colson. "Ultimate Limit Strength of Column-Base Connections." *Journal of Constructional Steel Research* 14, no. 4 (January 1989): 301–320. doi:10.1016/0143-974x(89)90041-2.
- [5] Ravari, Ali Karbakhsh, Ismail Bin Othman, and Zainah Binti Ibrahim. "Finite element analysis of bolted column base connection without and with stiffeners." *International Journal of Physical Sciences* 6, no. 1 (2011): 1-7.
- [6] Melchers, R.E. "Column-Base Response Under Applied Moment." *Journal of Constructional Steel Research* 23, no. 1–3 (January 1992): 127–143. doi:10.1016/0143-974x(92)90040-1.
- [7] Kontoleon, M.J., E.S. Mistakidis, C.C. Baniotopoulos, and P.D. Panagiotopoulos. "Parametric Analysis of the Structural Response of Steel Base Plate Connections." *Computers & Structures* 71, no. 1 (March 1999): 87–103. doi:10.1016/s0045-7949(98)00232-6.
- [8] Ermopoulos, John Ch., and George N. Stamatopoulos. "Mathematical Modelling of Column Base Plate Connections." *Journal of Constructional Steel Research* 36, no. 2 (January 1996): 79–100. doi:10.1016/0143-974x(95)00011-j.
- [9] Stamatopoulos, G.N., and J. Ch. Ermopoulos. "Experimental and Analytical Investigation of Steel Column Bases." *Journal of Constructional Steel Research* 67, no. 9 (September 2011): 1341–1357. doi:10.1016/j.jcsr.2011.03.007.
- [10] Dunai, László, Yuhshi Fukumoto, and Yasuhiro Ohtani. "Behaviour of Steel-to-Concrete Connections Under Combined Axial Force and Cyclic Bending." *Journal of Constructional Steel Research* 36, no. 2 (January 1996): 121–147. doi:10.1016/0143-

974x(95)00005-g.

- [11] Horová K, Tomšů J, Wald F. "To base plates of hollow sections columns". Department of Steel and Civil Structures, Czech Technical University in Prague; 2009.
- [12] Targowski, R., D. Lamblin, and G. Guerlement. "Baseplate Column Connection Under Bending: Experimental and Numerical Study." *Journal of Constructional Steel Research* 27, no. 1–3 (January 1993): 37–54. doi:10.1016/0143-974x(93)90005-d.
- [13] Khodaie, S., M.R. Mohamadi-shooreh, and M. Mofid. "Parametric Analyses on the Initial Stiffness of the SHS Column Base Plate Connections Using FEM." *Engineering Structures* 34 (January 2012): 363–370. doi:10.1016/j.engstruct.2011.09.026.
- [14] Krishnamurthy, Natarajan, and David P. Thambiratnam. "Finite Element Analysis of Column Base Plates." *Computers & Structures* 34, no. 2 (January 1990): 215–223. doi:10.1016/0045-7949(90)90364-8.
- [15] Gomez, Ivan, Amit Kanvinde, Chris Smith, and Gregory Deierlein. "Shear transfer in exposed column base plates." AISC report, University of California, Davis & Stanford University (2009).
- [16] Stamatopoulos, G.N., and J.Ch. Ermopoulos. "Interaction Curves for Column Base-Plate Connections." *Journal of Constructional Steel Research* 44, no. 1–2 (October 1997): 69–89. doi:10.1016/s0143-974x(97)00038-2.
- [17] Adany, S. "Numerical and experimental analysis of bolted end-plate joints under monotonic and cyclic loading." PhD diss., PhD Thesis. Budapest University of Tech Econom, Hungary, 2000.
- [18] Grilli, David, Robert Jones, and Amit Kanvinde. "Seismic Performance of Embedded Column Base Connections Subjected to Axial and Lateral Loads." *Journal of Structural Engineering* 143, no. 5 (May 2017): 04017010. doi:10.1061/(asce)st.1943-541x.0001741.
- [19] Freddi, Fabio, Christoforos A. Dimopoulos, and Theodore L. Karavasilis. "11.25: Rocking Damage-Free Steel Column Base with Friction Devices: Design Procedure and Global Seismic Response of Buildings." *Ce/papers* 1, no. 2–3 (September 2017): 3033–3042. doi:10.1002/cepa.355.
- [20] Zhang, Guowei, Peng Chen, Ziwei Zhao, and Jifeng Wu. "Experimental Study on Seismic Performance of Rocking Buckling-Restrained Brace Steel Frame with Lifiable Column Base." *Journal of Constructional Steel Research* 143 (April 2018): 291–306. doi:10.1016/j.jcsr.2018.01.002.
- [21] Baniotopoulos, Ch C., Z. Sokol, and F. Wald. "Column base connections." COST CI Report of WG6-Numerical simulation. Brussels-Luxemburg: European Commission (1999): 32–47.
- [22] Thambiratnam, David P., and N. Krishnamurthy. "Computer Analysis of Column Base Plates." *Computers & Structures* 33, no. 3 (1989): 839–850. doi:10.1016/0045-7949(89)90258-7.
- [23] Lim, Woo-Young, Dongkeun Lee, and Young-Chan You. "Exposed Column-Base Plate Strong-Axis Connections for Small-Size Steel Construction." *Journal of Constructional Steel Research* 137 (October 2017): 286–296. doi:10.1016/j.jcsr.2017.06.018.
- [24] Cui, Yao. "Shear Behavior of Exposed Column Base Connections." *Steel and Composite Structures* 21, no. 2 (June 10, 2016): 357–371. doi:10.12989/scs.2016.21.2.357.
- [25] Travush, Vladimir I., Anna S. Martirosyan, and Galina G. Kashevarova. "Computer Modeling as Evaluation Method of Column Base Bearing Capacity in Tower Buildings." *Procedia Engineering* 153 (2016): 773–780. doi:10.1016/j.proeng.2016.08.241.
- [26] Myers, A.T., A.M. Kanvinde, G.G. Deierlein, and B.V. Fell. "Effect of Weld Details on the Ductility of Steel Column Baseplate Connections." *Journal of Constructional Steel Research* 65, no. 6 (June 2009): 1366–1373. doi:10.1016/j.jcsr.2008.08.004.
- [27] Amit K, Deierlein G. Recent research on column base connections. *Proceedings of NASCC: The Steel Conference* 2011.
- [28] "Stahl-Eisen-Liste, 3. Auflage, Hrg.: Verein Deutscher Eisenhüttenleute, Düsseldorf, 1969." *Materialwissenschaft Und Werkstofftechnik* 2, no. 4 (June 1971): 223–224. doi:10.1002/mawe.19710020417.
- [29] DeWolf, John T., and D. Ricker. "Design of Column Base Plates." *American Institute of Steel Construction (AISC), Steel Design Guide Series* 1 (1990).
- [30] Blodgett, Omer W. "Design of welded structures." Cleveland: James F. Lincoln Arc Welding Foundation, 1966 (1966).
- [32] Shafieifar, Mohamadreza, Mahsa Farzad, and Atorod Azizinamini. "Experimental and Numerical Study on Mechanical Properties of Ultra High Performance Concrete (UHPC)." *Construction and Building Materials* 156 (December 2017): 402–411. doi:10.1016/j.conbuildmat.2017.08.170.
- [32] Farzad, Mahsa, Alireza Mohammadi, Mohamadreza Shafieifar, Huy Pham, and Atorod Azizinamini. "Development of Innovative Bridge Systems Utilizing Steel-Concrete-Steel Sandwich System." No. 17-02229. 2017.
- [33] Farzad, Mahsa, Mohamadreza Shafieifar, and Atorod Azizinamini. "Accelerated Retrofitting of Bridge Elements Subjected to Predominantly Axial Load Using UHPC Shell." No. 18-05067. 2018.
- [34] Shafieifar, Mohamadreza, Mahsa Farzad, and Atorod Azizinamini. "Alternative ABC Connection Utilizing UHPC." No. 17-03398. 2017.
- [35] Sadeghi, J., and M. Fesharaki. "Importance of nonlinearity of track support system in modeling of railway track dynamics." *International Journal of Structural Stability and Dynamics* 13, no. 01 (February 2013): 1350008. doi:10.1142/s0219455413500089.
- [36] Shafieifar, Mohamadreza, Mahsa Farzad, and Atorod Azizinamini. "A Comparison of Existing Analytical Methods to Predict the Flexural Capacity of Ultra High Performance Concrete (UHPC) Beams." *Construction and Building Materials* 172 (May 2018):

10–18. doi:10.1016/j.conbuildmat.2018.03.229.

[37] Momenzadeh, Seyedbabak, Onur Seker, Mahmoud Faytarouni, and Jay Shen. “Seismic Performance of All-Steel Buckling-Controlled Braces with Various Cross-Sections.” *Journal of Constructional Steel Research* 139 (December 2017): 44–61. doi:10.1016/j.jcsr.2017.09.003.

[38] Shen, Jay, Onur Seker, Bulent Akbas, Pinar Seker, Seyedbabak Momenzadeh, and Mahmoud Faytarouni. “Seismic Performance of Concentrically Braced Frames with and Without Brace Buckling.” *Engineering Structures* 141 (June 2017): 461–481. doi:10.1016/j.engstruct.2017.03.043.

[39] Tastani, S. P., and S. J. Pantazopoulou. “Experimental evaluation of the direct tension-pullout bond test.” *Bond in Concrete—from research to standards* (2002).